Lab on a Chip
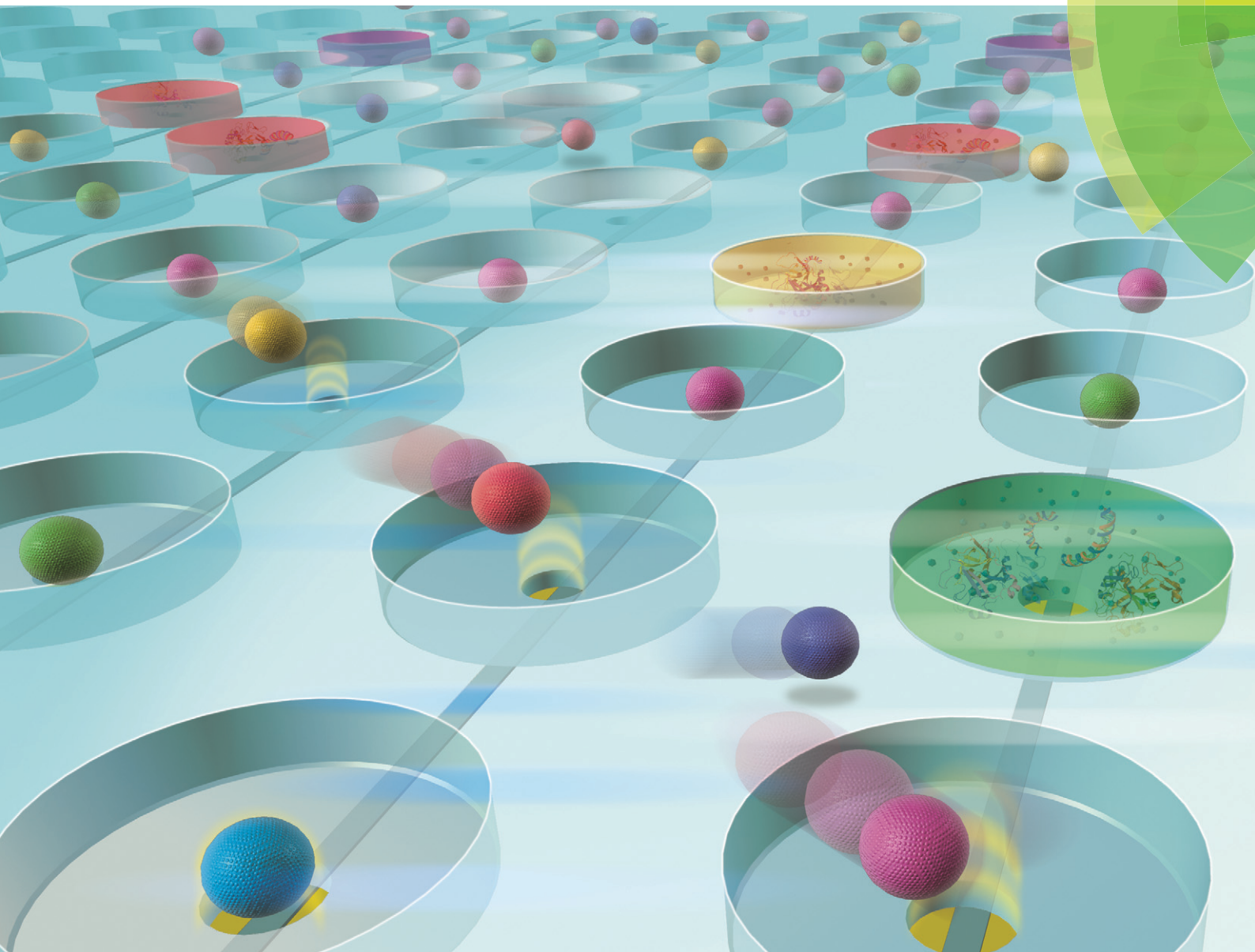
Miniaturisation for chemistry, physics, biology, materials science and bioengineering

www.rsc.org/loc

ROYAL SOCIETY OF CHEMISTRY

175 YEARS

PAPER
Soo Hyeon Kim and Teruo Fujii
Efficient analysis of a small number of cancer cells at the single-cell level using an electroactive double-well array

CrossMark
click for updates

Efficient analysis of a small number of cancer cells at the single-cell level using an electroactive double-well array†

Soo Hyeon Kim* and Teruo Fujii*

Analysis of the intracellular materials of a small number of cancer cells at the single-cell level is important to improve our understanding of cellular heterogeneity in rare cells. To analyze an extremely small number of cancer cells (less than hundreds of cells), an efficient system is required in order to analyze target cells with minimal sample loss. Here, we present a novel approach utilizing an advanced electroactive double-well array (EdWA) for on-chip analysis of a small number of cancer cells at the single-cell level with minimal loss of target cells. The EdWA consisted of cell-sized trap-wells for deterministic single-cell trapping using dielectrophoresis and high aspect ratio reaction-wells for confining the cell lysates extracted by lysing trapped single cells *via* electroporation. We demonstrated a highly efficient single-cell arraying (a cell capture efficiency of 96 ± 3%) by trapping diluted human prostate cancer cells (PC3 cells). On-chip single-cell analysis was performed by measuring the intracellular β-galactosidase (β-gal) activity after lysing the trapped single cells inside a tightly enclosed EdWA in the presence of a fluorogenic enzyme substrate. The PC3 cells showed large cell-to-cell variations in β-gal activity although they were cultured under the same conditions in a culture dish. This simple and effective system has great potential for high throughput single-cell analysis of rare cells.

Introduction

Single-cell analysis of a small number of cancer cells (*i.e.*, circulating tumor cells or cancer stem cells) is important to improve our understanding of tumor heterogeneity, which would contribute to various clinical applications, such as diagnosis, prognosis, and choice of therapy. For instance, identifying the circulating tumor cells' biological heterogeneity is required in order to predict drug response and resistance, and to monitor therapy response and the cancer recurrence rate.[1] A major issue with analyses of rare cells is that the target cells are extremely rare and mixed with other cell types. For instance, only 1–100 circulating tumor cells exist in 10 mL of blood, mixed with 10^{10} blood cells. Recently, microfluidics has been successfully employed for high-throughput and automatable isolation of rare cells by using the physical,[2–6] biochemical[7,8] or dielectric properties[9–11] of the target cells. However, an efficient method for the analysis of isolated target cells at the single-cell level has yet to be developed because of technical difficulties in manipulating an ex-

tremely small number of target cells (less than hundreds of cells). To analyze such a small number of target cells, a novel method that enables high efficiency single-cell capture and subsequent analysis of the intracellular materials of the captured cells needs to be developed.

Lab-on-a-chip technologies have been widely employed for the manipulation and analysis of single cells to understand the cellular heterogeneity in a cell population.[12] The use of cell-sized microwells in an array is the simplest method to array single cells by using gravity.[13,14] Dielectrophoresis (DEP) has been used for trapping and sorting individual cells.[15–17] Hydrodynamic single-cell arraying methods have been used to observe cellular responses, allowing a rapid change of biochemical reagents for various stimuli.[18–20] Recently, a significant improvement in single-cell trapping yield (97%) has been realized by optimizing the flow profiling.[21] However, these single-cell arraying techniques have only been applied for observing cellular responses to chemical stimuli. A microwell array, utilizing electrostatic functions including DEP for cell trapping and electroporation (EP) for cell lysis, was developed for arraying single *Escherichia coli* cells and lysing them to get intracellular materials.[22] However, the device could not be used for the analysis of the intracellular materials from single cells since confinement of the lysates of single cells was not technically possible; cell membrane disruption was immediately followed by diffusion of the cell lysates, causing

Institute of Industrial Science, The University of Tokyo, Japan.
E-mail: shkim@iis.u-tokyo.ac.jp, tfujii@iis.u-tokyo.ac.jp; Tel: +81 3 5452 6213,
+81 3 5452 6211

cross-contamination of the intracellular materials among each cell. To directly analyze intracellular materials within single cells, confinement of the intracellular contents is required to prevent cross-contamination and dilution of the intracellular materials after cell lysis.

Analysis of intracellular materials, such as nucleic acids and proteins, in single cells is required to study the molecular characteristics of target cells and their diverse biological functions. Multilayer polydimethylsiloxane (PDMS) microfluidic devices,[23–28] water-in-oil droplets,[29] and microfabricated structures[30] have been developed to confine and directly analyze the intracellular materials of single cells. A practical drawback of these approaches is the low throughput nature of the single cell trapping and lysing process. To improve the throughput, we developed an electroactive microwell array containing electrodes at the bottom of each microwell for trapping single cells by using DEP, followed by on-chip single-cell analysis after lysing the trapped cells by using EP.[31,32] Similar approaches utilizing arrayed microwells were developed for the analysis of intracellular materials of single cells.[33–36] Although previous methods successfully demonstrated the feasibility of on-chip single-cell analysis of intracellular materials, it is difficult to utilize these systems to analyze a small number of cells because of their exceedingly low cell capture efficiency. For instance, methods utilizing hydrodynamic cell traps have shown a low cell capture efficiency of approximately 1% (ref. 34) or 5% (ref. 37) because most cells were diverted around the trapping structure instead of flowing directly into it. Our previous electroactive microwell array[31,32] utilizing DEP for cell trapping also showed a low cell capture efficiency of 10% due to the relative thickness (15 μm) and moderate aspect ratio (diameter to thickness ratio) of the microwells. These factors prevented efficient cell delivery to the bottom of the microwells, where strong electric fields were formed. Because the number of target cells is extremely low in rare cancer cell analysis, improvement in cell capture efficiency is required for reliable single-cell analysis of the intracellular materials of a small number of cancer cells.

Here, we present a novel method utilizing an electroactive double-well array (EdWA) to achieve highly efficient single-cell trapping, followed by confinement and on-chip analysis of the intracellular materials from trapped single cells (Fig. 1). The cell capture efficiency was significantly improved by utilizing a high aspect ratio reaction-well fabricated on a thin trap-well, which allowed efficient cell delivery to the bottom of the well where the DEP force was the strongest. The tightly enclosed double-wells efficiently confined the intracellular materials from the single cells for subsequent on-chip analysis. Here, we report the validation of the EdWA device by performing electric and flow field simulations and evaluating the cell capture efficiency by trapping a small number of prostate cancer (PC3) cells. The feasibility of the EdWA for an on-chip single-cell analysis was demonstrated by measuring the intracellular β-galactosidase (β-gal) activity of the trapped single PC3 cells.

Working principles and design of the device

Dielectrophoresis for cell trapping

The electroactive microwells employed DEP to trap the target cells into electrodes patterned at the bottom of each microwell. The DEP force (F_{DEP}) acting on a spherical cell with a radius of a can be approximated by

$$F_{DEP} = 2\pi\varepsilon_e a^3 Re[K(2\pi f)]\nabla|E_e|^2, \tag{1}$$

$$K(2\pi f) = \frac{\varepsilon_{cell}^* - \varepsilon_e^*}{\varepsilon_{cell}^* + 2\varepsilon_e^*}, \tag{2}$$

where ε, f, and E_e are the permittivity, the frequency, and the amplitude of the electric field, respectively. The subscripts cell and e represent the cell and the suspending medium, and $\varepsilon^* = \varepsilon + \frac{\sigma}{2\pi f}j$ is the complex permittivity, where σ is the conductivity and $j = (-1)^{1/2}$. $Re[K(2\pi f)]$ is the real part of the polarization factor, called the real part of the Clausius–Mossotti (CM) factor. When the real part of the CM factor is larger than 0, cells are attracted toward the strong electric field (positive DEP (pDEP)). Conversely, when the real part of the CM factor is less than 0, cells are directed away from the strong electric field (negative DEP (nDEP)). The CM factor can be controlled by adjusting the conductivity of the external medium and the frequency of the applied electric fields.
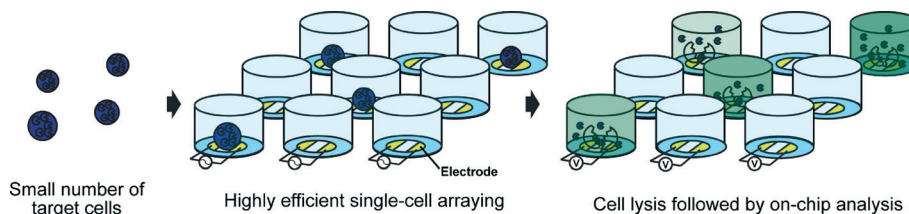

Fig. 1 A schematic illustration of the analysis of intracellular materials from single cells. A small number of cells were arrayed at the single-cell level with minimal target cell loss using DEP. The arrayed single cells were isolated inside tightly enclosed microreactors with assay reagents. Isolated single cells were lysed using EP and cell lysates were available to react with the assay reagents. Intracellular materials from the single cells were analyzed by measuring the signals from the reaction.

pDEP is widely used for the manipulation of mammalian cells due to the simple electrode design and strong DEP force that can be applied to the target cells. However, mammalian cells suspended in a culture medium typically show an nDEP response due to a high culture medium conductivity. In the present study, a sucrose-based low conductivity buffer was used to decrease the medium conductivity and to adjust the osmotic pressure. A high magnitude and positive real part of the CM factor was achieved at a megahertz-order electric field (Fig. S1†). Several demonstrations using a low conductivity buffer[38] showed no effect on cell viability during cell culture following cell trapping with pDEP.

Design of the electroactive double-well array

The EdWA was composed of a trap-well array for single-cell trapping and a reaction-well array for the confinement and analysis of lysates from single cells (Fig. 2A). Transparent electrodes were patterned on a glass substrate to induce electrostatic forces, including DEP and EP. The distance between electrodes was 8 μm, which was smaller than the target cell diameter (15 μm). To achieve single-cell resolution for

DEP trapping, thin trap-wells (20 μm in diameter) were fabricated on the electrodes using a photoresist, and aligned with the electrodes in order to place a pair of electrodes (anode and cathode) at the bottom of the trap-wells. The trap-well array structure efficiently blocked the electric fields except for the area where the trap-wells were patterned. Additionally, high aspect ratio reaction-wells (11 μm in height) were fabricated on the trap-wells using a photoresist to prevent collapse of the trapped cells during the double-well closing process. Tightly enclosed double-wells efficiently confined the intracellular materials from single cells after lysis using EP (Fig. 2B). The high aspect ratio of the reaction-well allowed efficient target cell delivery towards the bottom of the double-wells where the DEP force was the strongest.

To improve the cell capture efficiency, the double-wells were obliquely-arranged and the cells were focused at the center stream using the sheath flow that was generated in the microfluidic channel (Fig. 2C). In the present EdWA, only the cells flowing to the double-wells could be trapped in the double-wells since the electric fields formed on the double-wells and were efficiently blocked between the double-wells
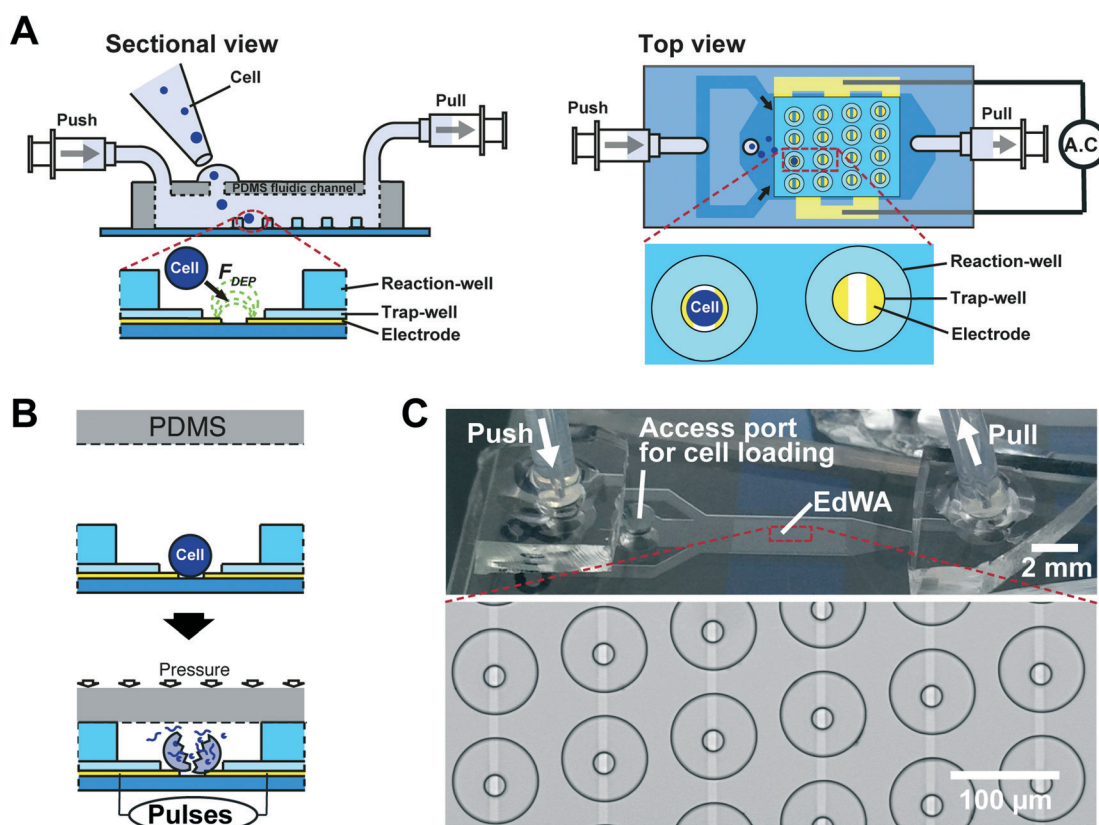

Fig. 2 Design of the EdWA and the fabricated device. (A) A schematic illustration of the device. Each double-well had patterned electrodes at the bottom of the trap-well to induce DEP for cell trapping. Thin trap-wells and high aspect ratio reaction-wells were fabricated on the patterned electrodes. The trap-wells had a diameter comparable to that of the cells, which allowed deterministic single-cell trapping. (B) Confinement of intracellular materials from single cells. The double-wells were tightly enclosed by pressing a PDMS membrane onto the EdWA. The reaction-well protected the trapped single cells from collapsing during the well-closing process. The trapped single cells were lysed using EP and the intracellular materials from the cells were confined to the enclosed EdWA for a downstream on-chip assay. (C) A photo of the fabricated EdWA. The EdWA substrate was assembled with a PDMS microfluidic channel that had an access port for sample injection and side channels to focus injected cells into the center of the EdWA with sheath flow. The double-wells were obliquely-arranged to efficiently trap cells that flowed over the EdWA. The array contained 1464 double-wells inside a 17 mm² area.

by an insulation layer. By arranging the double-wells obliquely in an array, the cells efficiently flowed onto the double-wells. Moreover, the cells flowing between the EdWA and the side walls of the microfluidics channel could not be trapped since there were no electrodes between the EdWA and the side walls of the microfluidic channel. To solve this problem, the sheath flow was induced by the flow from the side channels to focus the cells at the center stream of the microfluidic channel.

Materials and methods

Device fabrication

The EdWA was fabricated using conventional photolithography and etching processes.[31] First, the shape of the electrodes was patterned on an indium tin oxide (ITO)-coated glass substrate (GEOMATEC Co., Japan) by using a positive-type photoresist (S1813; Shipley Far Ltd., USA). S1813 was deposited onto the clean ITO glass using a spin coater. Here, the photoresist was spread onto the ITO glass at 500 rpm for 10 s and then increased to 4000 rpm at an acceleration of 700 rpm per second. The ITO glass substrate was then soft-baked at 120 °C for 2 min. After baking, a chromium photo-mask, which was patterned for the interdigitated electrode, was applied to the photoresist-coated ITO glass and exposed to ultraviolet light. Subsequently, the resist was developed using a developer (AZ developer; AZ Electronic Materials) for 2 min, and the ITO glass was rinsed with deionized water. The ITO was etched with an etchant (ITO-02; KANTO KAGAKU Co., Japan) for 5 min at 40 °C. Afterwards, the substrate was cleaned and rinsed with acetone and isopropyl alcohol to remove the photoresist layer that remained on the substrate. To fabricate a trap-well array on the patterned electrodes, the patterned ITO electrodes were coated with a negative-type photoresist (SU-8 3005; MicroChem Co., USA). Here, SU-8 3005 was spread onto the electrode substrate at 500 rpm for 10 s and then raised to 4000 rpm at an acceleration of 700 rpm per second, to a thickness of 4 μm. To fabricate thick trap-wells for the evaluation of thickness-dependent cell capture efficiency, a negative-type photoresist SU-8 3010 (MicroChem Co., USA) was spread at 500 rpm for 10 s and then increased to 3000 and 1000 rpm to fabricate the 9 and 17 μm trap-wells, respectively. The photoresist-coated electrode substrate was then soft-baked at 95 °C for 2 min. A chromium photo-mask patterned for the trap-well array was aligned with the patterned ITO electrodes and exposed to ultraviolet light. The substrate was then post-exposure baked at 95 °C for 1 min, and was subsequently developed for 2 min using an SU-8 developer (propylene glycol monomethylether acetate; GODO Co. Ltd., Japan) and rinsed with isopropyl alcohol (Wako Pure Chemical Industries, Ltd., Japan). To fabricate additional reaction-wells on the trap-wells, the trap-well substrate was coated with SU-8 3010 by spreading it at 500 rpm for 10 s, which was then increased to 2800 rpm at an acceleration of 460 rpm per second, to a thickness of 11 μm. The substrate was then soft-baked at 95

°C for 4 min. A chromium photo-mask patterned for the reaction-well array was aligned with the trap-well array substrate and exposed to ultraviolet light. The substrate was then post-exposure baked at 95 °C for 2 min, and subsequently developed for 4 min using an SU-8 developer and rinsed with isopropyl alcohol.

The microfluidic channel for the EdWA was fabricated by using PDMS (Silopt 184; Dow Corning Toray Co. Ltd.) through a standard replica molding process. A mold master was fabricated with a negative-type photoresist (SU-8 3035, MicroChem Co., USA). SU-8 3035 was spread onto a silicon wafer at 500 rpm for 10 s, which was then increased to 2000 rpm at an acceleration of 400 rpm per second, to a thickness of 50 μm. The wafer was then soft baked at 95 °C for 15 min. A chromium photo-mask patterned for the fluidic channel was applied to the silicon wafer and exposed to ultraviolet light. The wafer was then post-exposure baked at 95 °C for 5 min, and subsequently developed for 8 min using an SU-8 developer and rinsed with isopropyl alcohol. To allow easy release of the PDMS replica, the mold master was exposed to CHF_3 plasma and coated with a fluorocarbon layer using a reactive-ion etching machine (RIE-10NR; Samco Co., Japan). A PDMS prepolymer was mixed with a curing reagent (at a 10 : 1 mass ratio) and poured into the mold master. The mixture was incubated in a desiccator at approximately 0.02 MPa for 30 min to remove bubbles from the PDMS prepolymer. Subsequently, the PDMS was cured at 75 °C for 2 h and polymerized PDMS was then removed from the mold. The height and width of the microfluidic channel were 50 and 3600 μm, respectively. Thereafter, holes were made to serve as access ports to the flow channels.

The PDMS channel and the EdWA substrate were exposed to O_2 plasma using a reactive-ion etching machine and bonded together. Before use, the device was washed with ethanol and water to prevent air bubbles in the double-wells; subsequently, the wells were filled with a low conductivity buffer.

Cells and reagents

The PC3 human prostate cancer cell line (obtained from the RIKEN Bio Resource Center, Japan) was used for this demonstration. The PC3 cells were cultured in a humidified incubator (37 °C in an atmosphere of 5% CO_2). The culture medium was RPMI 1640 (Invitrogen, USA) supplemented with fetal bovine serum (10%; Gemini Bio-products, USA) and penicillin–streptomycin (1%; Sigma Chemical Co., USA). To adjust the conductivity of the cell suspension medium, a low conductivity buffer (10 mM HEPES, 0.1 mM $CaCl_2$, 59 mM D-glucose and 236 mM sucrose) was used. Bovine serum albumin (BSA; Sigma Chemical Co., USA) was added to the low conductivity buffer to block nonspecific cell adhesion (2% w/v). The final conductivity of the buffer was 22.4 mS m^{-1}. An enzymatic assay for intracellular β-gal was carried out using a fluorogenic β-gal substrate, fluorescein-di-β-D-galactopyranoside (FDG; Marker Gene Technologies, Inc, USA).

Experimental setup

The device was placed on an x–y translational stage located on an inverted microscope (IX 71; Olympus, Japan). Cells trapped in the device were monitored with a digital CCD camera (ORCA-R2; Hamamatsu Photonics, Japan) installed on the microscope. Electric potentials for DEP trapping and EP lysis were applied to the ITO electrodes by using a function generator (WF1948; NF Corp., Japan) through an amplifier (HSA4101; NF Corp., Japan). The EdWA was closed tightly by applying a pressure to the PDMS membrane by using a rounded plastic tip connected to a motorized stage (SGAM20; Sigma Koki Co. Ltd., Japan) controlled by a stage controller (SHOT-202AM; Sigma Koki Co. Ltd., Japan). Gastight glass syringes (Hamilton Company, USA), connected to the outlet or the side channel, were mounted on precisely controlled syringe pumps (MFS-SP1; Microfluidic System Works Inc., Japan).

Cell trapping

Cultured PC3 cells were stained with a blue fluorescent probe (CellTracker Blue CMAC; Invitrogen, USA) or a green fluorescent probe (Calcein AM; Wako Pure Chemical Industries Ltd., Japan) and subsequently harvested. Before cells were injected into the device, the culture medium was gently removed following centrifugation at $190 \times g$ for 3 min, and the low conductivity buffer was added to adjust the conductivity of the

cell suspension medium in order to induce a positive DEP. A wide range of cell concentrations, from 2.7×10^4 to 2.2×10^5 cells per mL, was used for this demonstration. To calculate the cell capture efficiency, 2 μL of the cell suspension was taken using a pipet and dropped onto a microscope glass slide. Cells on the slide were counted, and 53–433 cells were used for the study. The same volume of cell suspension was loaded into the device trough the access port. Cells were delivered into the microfluidic channel by applying a negative pressure induced by the syringe connected to the microfluidic channel outlet. To generate the sheath flow, a positive pressure was induced by using the syringe connected to the side channel. Cells were trapped into the electroactive microwells by applying electric potentials to the ITO electrodes. Fluorescence images for the microwells were acquired after cell trapping, and the trapped cells were counted.

Results

Trap-well array for high cell capture efficiency

To improve the inherent cell capture efficiency of the electroactive microwells, we investigated the DEP force magnitude dependence on the microwell thickness. Commercially available codes (Comsol Multiphysics, COMSOL group, USA) were used to simulate electric fields forming in the electroactive microwells. Fig. 3A shows the simulated electric field
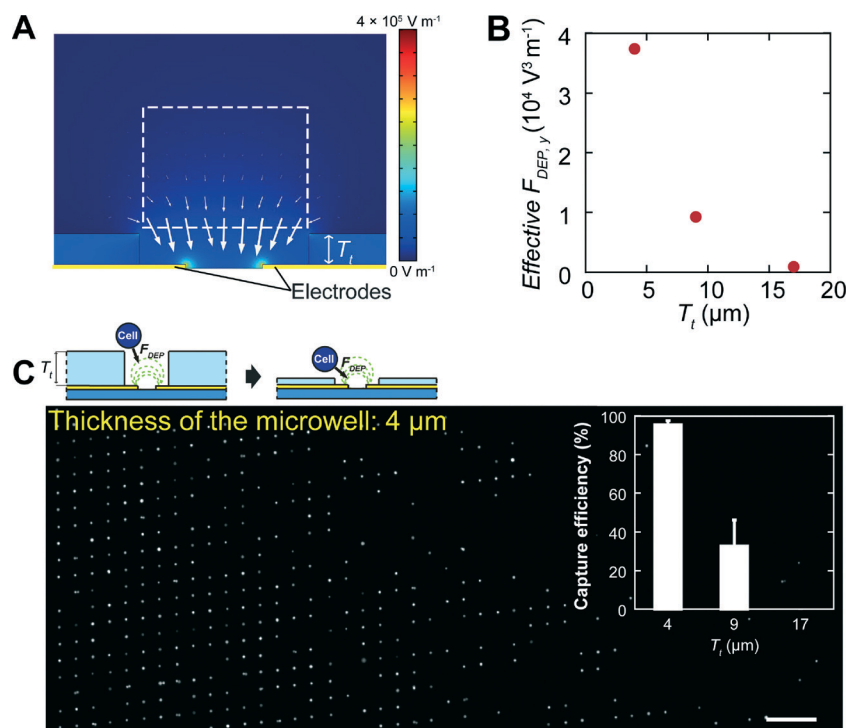

Fig. 3 Single-cell trapping using a trap-well array. (A) Simulated contours of the electric field (E_e) and vectors of the electric field gradient ($\nabla|E_e|^2$). Electric potentials were assigned at the electrode boundaries. The $\nabla|E_e|^2$ vectors were directed towards the inside of the well and the magnitude of $\nabla|E_e|^2$ decreased with increased distance from the electrodes. (B) The magnitude of effective $F_{DEP,y}$ as a function of well thickness. The effective $F_{DEP,y}$ significantly decreased with increased microwell thickness. In the current study, 4, 9, and 17 μm-thick microwells were investigated. (C) A fluorescence image of a 4 μm trap-well array following cell trapping. Here, 433 cells were introduced and 405 cells were trapped in the trap-well array, where 27% of the microwells were occupied by the cells. Scale bar is 300 μm. The inset shows the dependence of cell capture efficiency on the thickness of the trap-well array. Cell capture efficiency decreased with increased trap-well thickness.

strength (E_e) contours and gradient of the electric field strength ($\nabla|E_e|^2$) vectors. The magnitude of $\nabla|E_e|^2$, which is proportional to the magnitude of the DEP force, decreased with increased distance from the electrodes. To evaluate the DEP force acting on a cell, we accounted for the effective $F_{DEP,y}$, which is defined by

$$\text{effective } F_{DEP,y} = \int_{\Omega} \left(\frac{\partial |E_e|^2}{\partial y} \right) ds$$

where Ω represents the area of a white dotted rectangle above the microwell in Fig. 3A. The effective $F_{DEP,y}$ represents the magnitude of the attractive DEP force acting on a cell when it flowed over the microwells. Microwell thicknesses of 4, 9, and 17 μm were investigated. The effective $F_{DEP,y}$ dramatically decreased with the microwell thickness (Fig. 3B). Simulation results indicated that a cell flowing over the thin trap-wells was exposed to a strong $\nabla|E_e|^2$, allowing efficient cell trapping using DEP.

To investigate the effect of well thickness on cell trapping, we trapped PC3 cells by using a trap-well array with various thicknesses of (4, 9, and 17 μm). Diluted PC3 cells were introduced into the access port of the microfluidic device and delivered using a negative pressure at a flow rate of 2 μL min⁻¹. To focus the cells to the center of the microwell array with sheath flow, a positive pressure was applied to the side channel at a flow rate of 0.5 μL min⁻¹. The cells were trapped in the trap-well using a positive DEP by applying a sinusoidal electric potential (peak-to-peak voltage, Vpp = 4 V and f = 8 MHz) to the electrodes. An improved cell capture efficiency (a percentage ratio of the number of trapped cells to the number of cells introduced) of 95 ± 2.1% was obtained using the 4 μm trap-well array (Fig. 3C). However, the cell capture efficiency decreased with the increase in trap-well thickness, where the cell capture efficiency was 33 ± 13% and 0 ± 0% for the 9 and 17 μm trap-wells, respectively. Even though a high electrical potential of 15 V was applied, a cell capture efficiency of only 19 ± 8.9% was obtained for the 17 μm trap-well. These results indicate that the thin trap-well array is effective for obtaining efficient DEP trapping because the cells are exposed to a strong DEP force as they flow over the thin trap-well array.

Single cell trapping with EdWA

Confinement of intracellular materials from single cells after lysis is required for direct analysis of the cellular contents. Although the 4 μm trap-well array showed an impressive cell capture efficiency, the trapped cells were ruptured during the well closing process because the PDMS membrane was directly pressing on the trapped cells. This caused mechanical lysis of the cells prior to closing (data not shown). To protect the trapped cells and confine the intracellular materials from each cell, a high aspect ratio reaction-well was fabricated on the trap-wells. The high aspect ratio of the reaction-well allowed efficient delivery of the target cells to the bottom of the microwells, where the DEP force was the strongest. Flow

field dependency on the aspect ratio of the microwells was investigated by performing 2D simulations of flow fields by using commercially available codes. Fig. 4A shows simulated velocity field contours and streamlines. Streamlines for the high aspect ratio microwells penetrated the microwell and few reached the bottom of the microwell. The simulation result indicated that the target cells flowing over the high aspect ratio microwells were exposed to a strong attractive DEP force because they penetrated and reached the bottom of the microwell where the electrodes were patterned.

The cell capture efficiency of the EdWA was evaluated by trapping a small number of PC3 cells in reaction-wells of varying diameters (40, 80, and 160 μm) and fixed thickness (11 μm), which were fabricated on the 4 μm trap-wells. Diluted PC3 cells were introduced into the device at a flow rate of 2 μL min⁻¹. No cells were trapped inside the double-wells in the absence of DEP force. Cells were trapped in the EdWA system by applying a sinusoidal electric potential (Vpp = 5 V and f = 8 MHz) to the electrodes. The EdWA required slightly higher electric fields than the trap-well array for efficient single cell trappings. The trap-wells were gradually occupied by single cells from the upstream microfluidic channel (Fig. 4B and Supplementary movie†). The diameter of the trap-wells (20 μm) was comparable to that of the target cells (15 μm); therefore, when a trap-well was occupied with a single cell, a second cell was prevented from entering due to space restrictions. The EdWA showed good cell capture efficiencies of 96 ± 2.8%, 95 ± 2.1%, and 83 ± 4.4% for reaction-wells 160, 80, and 40 μm in diameter, respectively (Fig. 4C). The wide reaction-well array showed a slightly improved cell capture efficiency because the cells were more efficiently delivered to the bottom of the double-wells.

Confinement of intracellular materials from single cells

Trapped single cells were lysed inside the tightly enclosed EdWA microwells to confine the intracellular materials from the trapped single cells for downstream analysis. The EdWA was closed to prevent cross contamination during the cell lysis process by gently pressing the PDMS membrane against the double-well array substrate by using a motorized manipulator. When the PDMS membrane was in contact with the double-well array, the image of the double-well array started to lose its focus. Then, we further pushed the PDMS membrane for another 50 μm to tightly enclose the EdWA. The trapped cells emitted a clear fluorescence signal inside the tightly enclosed EdWA with no extracellular fluorescence leakage observed (Fig. 5A), indicating an intact cell membrane inside the EdWA. The trapped cells were lysed by applying a series of bipolar pulses (Vpp = 100 V and f = 100 KHz) for 10 ms. Subsequently, cell membrane disruption was visualized by observing the release of fluorescent molecules from the cell (Fig. 5A). The fluorescence signal from each cell was confined to the tightly enclosed double-wells. Normalized fluorescence intensities significantly decreased (91 ± 4%) after pulsing (Fig. 5B), indicating that the trapped cells were efficiently lysed using EP due to pDEP-mediated
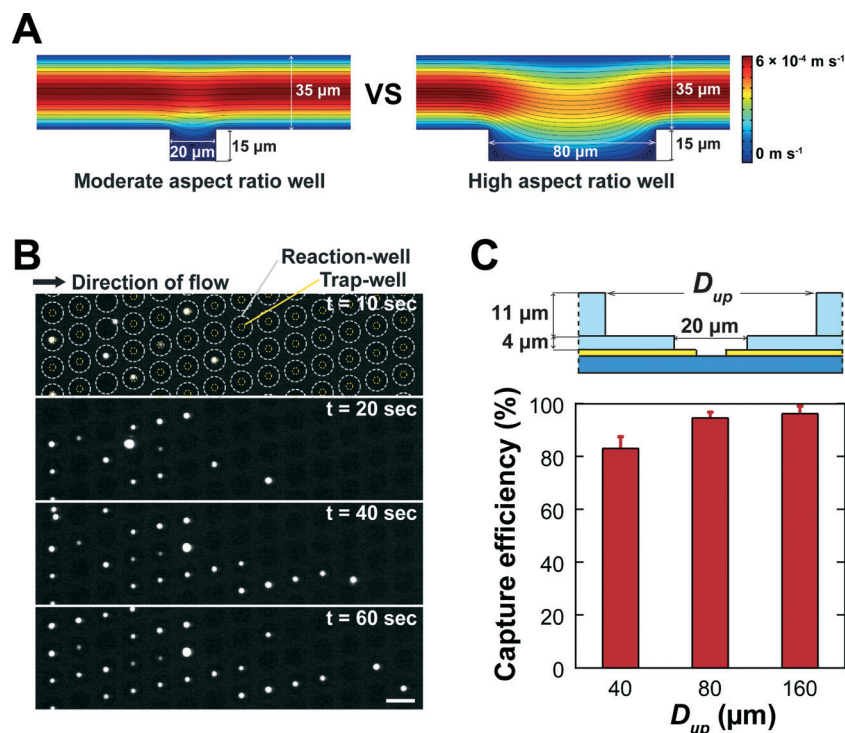
Fig. 4 Single-cell trapping using an EdWA. (A) Simulated contours of the flow velocity and streamlines of moderate and high aspect ratio microwells. Streamlines of a moderate aspect ratio microwell did not penetrate the microwell whereas those of a high aspect ratio microwell did. (B) Time-lapse images of an EdWA during PC3 trapping (a part of the Supplementary movie†). Yellow and gray dashed-circles indicate the positions of the trap- and reaction-wells, respectively. Cells flowing onto the EdWA were attracted to the electrodes at the bottom of the trap-wells (yellow dotted circles) by a positive DEP force. When a cell occupied a trap-well, a second cell was prevented from entering the same well due to space restriction. Scale bar is 100 μm. (C) Cell capture efficiency as a function of the reaction-well diameter (D_{up}). The cell capture efficiency gradually increased with increased D_{up} because cells were more efficiently delivered to the bottom of the wide reaction-wells.

entrapment of cells on the edge of the electrodes where the electric field strength was the greatest.
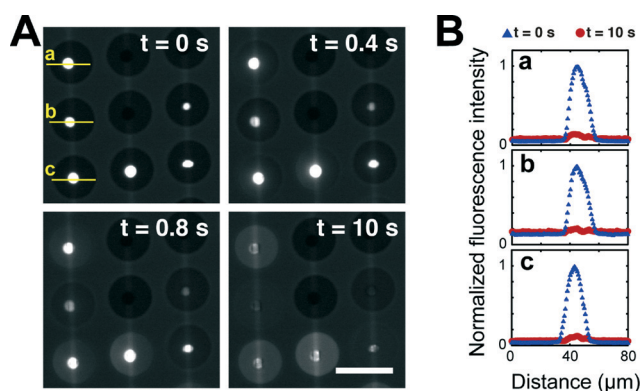

Fig. 5 Cell lysis inside a tightly enclosed EdWA. (A) Time-lapse images of an EdWA during PC3 cell lysis. The EdWA was tightly closed following cell trapping by pressing a PDMS membrane against the EdWA substrate. The reaction-well effectively protected the trapped cells during the well closing process. The trapped cells were lysed by applying strong electric potentials to the electrodes. The tightly enclosed reaction-well confined the intracellular materials from the single cells in a small volume without cross contamination from other wells. Scale bar is 100 μm. (B) Changes in fluorescence intensity due to cell lysis. The fluorescence intensity values were obtained along the indicated yellow lines inside the closed EdWA shown in A. The fluorescence intensities were normalized to local maxima.

The high aspect ratio reaction-wells on trap-wells physically protected the trapped cells during the EdWA closing process without affecting the cell capture efficiency. This feature allowed highly efficient single cell trapping, followed by confinement of the intracellular materials with minimal sample loss. The reaction volume for the downstream single-cell analysis can be easily adjusted by changing the reaction-well diameter. The reaction-well diameter determines the dilution of intracellular materials when cells are lysed inside the EdWA. A large reaction-well diameter would decrease the number of available double-wells within the limited area. Hence, the size of the reaction-well should be determined by accounting for the amount of target cells needed for the analysis as well as intracellular material dilution for downstream analysis.

Intracellular enzymatic assay at the single-cell level using the EdWA

A direct analysis of the individual cellular contents within the EdWA was demonstrated by measuring the intracellular β-gal activity in the single cell lysates. Diluted PC3 cells were stained with a fluorescent probe, CellTracker Blue, and were introduced into the device and trapped within the EdWA. The low-conductivity buffer was replaced by a buffer containing a fluorogenic β-gal substrate (FDG; 1 mM). After closing the EdWA by pressing the PDMS membrane, the

electric fields for DEP were turned off, and the trapped cells were lysed by applying a series of bipolar pulses (Vpp = 100 V and f = 100 KHz) for 10 ms. The pulses did not appear to affect β-gal activity (Fig. S2†). Cell membrane disruption caused by the EP pulses released the intracellular β-gal that subsequently reacted with FDG, resulting in increased fluorescein fluorescence intensity (emission at 515 nm) from each enclosed double-well containing PC3 cell (Fig. 6A). No increase in fluorescence intensity was observed in empty double-wells. Leakage of fluorescein to the outside of the closed double-wells was not observed, as any leakage would have resulted in a homogeneous fluorescence intensity of the array. This result indicated that the EdWA was tightly closed and intracellular materials from single cells were efficiently isolated. The fluorescence intensity from each double-well was tracked over the course of a 25 min period and plotted (Fig. 6B). The β-gal enzymatic activity in the cell lysates was calculated from the slope of the plot. Fig. 6C shows the distribution of the intracellular β-gal activity in a PC3 cell population. We determined the double-wells that were vacant or occupied by two cells by observing images taken immediately before cell lysis, and excluded them from the analysis. The PC3 cells showed large cell-to-cell variations in intracellular β-gal activity, despite being cultured under the same conditions.

The EdWA allowed highly sensitive measurement of intracellular β-gal activity in the lysates of single cells. The tightly enclosed EdWA was able to confine intracellular β-gal molecules within an ultra-small volume (56 pL) and prevent cross contaminations with intracellular materials from other cells.

Moreover, because fluorescein molecules accumulated within the homogeneous and small volume of the EdWA, highly sensitive detection and measurement of the intracellular β-gal activity were permitted, even from single cells.

Discussion

Microfluidic approaches have been widely utilized in the analysis of intracellular materials from single cells by confining cellular contents in small reaction volumes. Arraying individual cells at predefined positions, the first and critical step of the isolation process, has been accomplished by using additional forces such as hydrodynamic force[34,35,37] and gravity.[33] However, previous systems showed low cell capture efficiencies because these methods were not able to actively attract target cells to the predefined positions. For instance, Eyer *et al.* utilized hydrodynamic cell traps; however, they achieved low cell capture efficiency because most cells did not flow straight into the trapping structure but were diverted around it.[34,35] Another method using gravity, introduced by Lee *et al.*, also showed a low cell capture efficiency because a significant number of cells settled down between the microwells and were flushed out.[33] Our method, which employs electroactive double-wells, was able to actively attract target cells because the DEP force was highly localized towards the bottom of the wells. This active trapping strategy, together with an optimized microwell design, allowed us to obtain high cell capture efficiency.

A significant improvement in the cell capture efficiency of the EdWA was achieved by separating the geometry of the
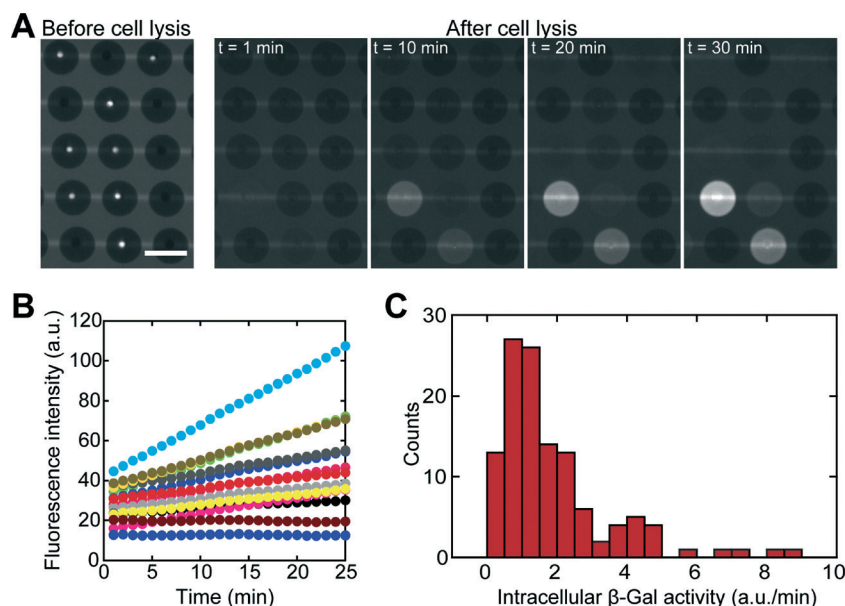

Fig. 6 Single cell enzymatic assay of PC3 cells by using an EdWA. (A) Representative fluorescence images of the single-cell enzymatic assay. A fluorescence image of trapped cells in an enclosed EdWA was acquired using a blue emission filter (466 nm) before cell lysis to determine the presence of a cell inside the EdWA. The trapped cells were lysed inside the tightly enclosed EdWA in the presence of FDG, a fluorogenic substrate of β-gal. Post-lysis fluorescence images of the EdWA were acquired using a green emission filter (515 nm) to monitor the presence of the fluorescent product (fluorescein) from FDG hydrolysis by intracellular β-gal. (B) Kinetics of the average fluorescence intensity from each double-well. (C) Distribution of the intracellular β-gal activity from each cell. Intracellular β-gal activities of single cells were determined from slopes of the plot shown in B.

microwells into a set of trap- and reaction-wells according to their functions—single-cell trapping and confinement of cell lysates. The cell-sized diameter of the microwell was required to achieve single-cell resolution of DEP cell trapping. The thickness of the microwell should be larger than the diameter of the target cells to protect the cells during the microwell closing process. In the previous version of electroactive microwells,[31,32] both functions were performed using a single microwell; therefore, the diameter and thickness of the microwell were comparable to the diameter of the target cell. However, this moderate aspect ratio of the microwells resulted in low cell capture efficiency because the cells were not efficiently delivered to the bottom of the microwells. In the present EdWA, functions of the microwells were segregated by using a double-well strategy—trap-wells for trapping single cells and reaction-wells for confining the cell lysates. This separation allowed us to optimize the size of each microwell; the trap-well thickness was optimized to improve the DEP force, whereas the reaction-well diameter was optimized for efficient cell delivery. These optimizations led to improved cell capture efficiency using a high aspect ratio reaction-well on a thin trap-well.

Further improvement in the cell capture efficiency can be achieved by actively recruiting cells to the surface of the double-well array. Since the DEP force significantly decreases with an increase in distance from the electrodes, it is important to control the cell's vertical position in the channel to maximize the DEP force acting on the cell. In the present system, cells loaded through an access port settled to the bottom of the channel by gravity as they flowed in. The use of an additional mechanism, such as using a vertical sheath flow to push the cell stream down,[39] may further improve the cell capture efficiency by effectively decreasing the cell–electrode distance.

The unique features of the EdWA would be beneficial for addressing a critical issue in the analysis of clinical samples. Due to limitations of clinical samples (*i.e.*, limited circulating tumor cell numbers and the ability to grow them in culture), more target cells need to be analyzed to detect the population heterogeneity and for successful implementation in clinical applications such as diagnosis, prognosis, and choice of therapy. We believe that our system is broadly applicable for the analysis of low-abundance clinical samples, due to its ability to confine and analyze intracellular materials from single cells with minimal target cell loss. To further assess the feasibility of the device, we plan to integrate a cell-concentrating[40] or cell-sorting microfluidic system directly upstream of the EdWA device to concentrate and isolate specific cell populations from blood based on their physical properties.

Conclusions

In this report, we have presented a microfluidic device that uses an EdWA for an on-chip analysis of intracellular materials from single cells with minimal sample loss. The feasibility of the EdWA device was demonstrated by arraying a small number of cancer cells with high cell capture efficiency followed by an intracellular enzymatic assay at the single-cell level. We believe that the EdWA can be efficiently used for the analysis of rare cells by addressing a critical issue in rare cell analysis: the loss of low-abundance cells. The combination of the EdWA with comprehensive analytical assays will assure highly sensitive and parallel analyses of rare cells for basic studies as well as clinical applications.

Acknowledgements

References

1 S. Bhatia, J. V. Frangioni, R. M. Hoffman, A. J. Iafrate and K. Polyak, *Nat. Biotechnol.*, 2012, **30**, 604–610.
2 E. Sollier, D. E. Go, J. Che, D. R. Gossett, S. O'Byrne, W. M. Weaver, N. Kummer, M. Rettig, J. Goldman, N. Nickols, S. McCloskey, R. P. Kulkarni and D. Di Carlo, *Lab Chip*, 2014, **14**, 63–77.
3 H. W. Hou, M. E. Warkiani, B. L. Khoo, Z. R. Li, R. A. Soo, D. S. Tan, W. T. Lim, J. Han, A. A. Bhagat and C. T. Lim, *Sci. Rep.*, 2013, **3**, 1259.
4 P. Augustsson, C. Magnusson, M. Nordin, H. Lilja and T. Laurell, *Anal. Chem.*, 2012, **84**, 7954–7962.
5 M. Antfolk, C. Antfolk, H. Lilja, T. Laurell and P. Augustsson, *Lab Chip*, 2015, **15**, 2102–2109.
6 P. Li, Z. Mao, Z. Peng, L. Zhou, Y. Chen, P. H. Huang, C. I. Truica, J. J. Drabick, W. S. El-Deiry, M. Dao, S. Suresh and T. J. Huang, *Proc. Natl. Acad. Sci. U. S. A.*, 2015, **112**, 4970–4975.
7 N. M. Karabacak, P. S. Spuhler, F. Fachin, E. J. Lim, V. Pai, E. Ozkumur, J. M. Martel, N. Kojic, K. Smith, P. I. Chen, J. Yang, H. Hwang, B. Morgan, J. Trautwein, T. A. Barber, S. L. Stott, S. Maheswaran, R. Kapur, D. A. Haber and M. Toner, *Nat. Protoc.*, 2014, **9**, 694–710.
8 S. Choi, O. Levy, M. B. Coelho, J. M. Cabral, J. M. Karp and R. Karnik, *Lab Chip*, 2014, **14**, 161–166.
9 P. R. Gascoyne, J. Noshari, T. J. Anderson and F. F. Becker, *Electrophoresis*, 2009, **30**, 1388–1398.
10 S. Shim, K. Stemke-Hale, A. M. Tsimberidou, J. Noshari, T. E. Anderson and P. R. Gascoyne, *Biomicrofluidics*, 2013, **7**, 11807.
11 H. S. Moon, K. Kwon, S. I. Kim, H. Han, J. Sohn, S. Lee and H. I. Jung, *Lab Chip*, 2011, **11**, 1118–1125.
12 C. E. Sims and N. L. Allbritton, *Lab Chip*, 2007, **7**, 423–440.
13 J. R. Rettig and A. Folch, *Anal. Chem.*, 2005, **77**, 5628–5634.
14 Y. Tokimitsu, H. Kishi, S. Kondo, R. Honda, K. Tajiri, K. Motoki, T. Ozawa, S. Kadowaki, T. Obata, S. Fujiki, C. Tateno, H. Takaishi, K. Chayama, K. Yoshizato, E. Tamiya, T. Sugiyama and A. Muraguchi, *Cytometry, Part A*, 2007, **71**, 1003–1010.

15 B. M. Taff and J. Voldman, *Anal. Chem.*, 2005, 77, 7976–7983.

16 N. Mittal, A. Rosenthal and J. Voldman, *Lab Chip*, 2007, 7, 1146–1153.

17 K. W. Huang, Y. C. Wu, J. A. Lee and P. Y. Chiou, *Lab Chip*, 2013, **13**, 3721–3727.

18 D. Di Carlo, L. Y. Wu and L. P. Lee, *Lab Chip*, 2006, **6**, 1445–1449.

19 D. Di Carlo, N. Aghdam and L. P. Lee, *Anal. Chem.*, 2006, 78, 4925–4930.

20 D. Wlodkowic, S. Faley, M. Zagnoni, J. P. Wikswo and J. M. Cooper, *Anal. Chem.*, 2009, **81**, 5517–5523.

21 S. Kobel, A. Valero, J. Latt, P. Renaud and M. Lutolf, *Lab Chip*, 2010, **10**, 857–863.

22 S. H. Kim, T. Yamamoto, D. Fourmy and T. Fujii, *Biomicrofluidics*, 2011, **5**, 24114.

23 J. W. Hong, V. Studer, G. Hang, W. F. Anderson and S. R. Quake, *Nat. Biotechnol.*, 2004, **22**, 435–439.

24 H. Wu, A. Wheeler and R. N. Zare, *Proc. Natl. Acad. Sci. U. S. A.*, 2004, **101**, 12809–12813.

25 Y. Marcy, C. Ouverney, E. M. Bik, T. Losekann, N. Ivanova, H. G. Martin, E. Szeto, D. Platt, P. Hugenholtz, D. A. Relman and S. R. Quake, *Proc. Natl. Acad. Sci. U. S. A.*, 2007, **104**, 11889–11894.

26 J. F. Zhong, Y. Chen, J. S. Marcus, A. Scherer, S. R. Quake, C. R. Taylor and L. P. Weiner, *Lab Chip*, 2008, **8**, 68–74.

27 N. Bontoux, L. Dauphinot, T. Vitalis, V. Studer, Y. Chen, J. Rossier and M. C. Potier, *Lab Chip*, 2008, **8**, 443–450.

28 H. C. Fan, J. Wang, A. Potanina and S. R. Quake, *Nat. Biotechnol.*, 2011, **29**, 51–57.

29 M. He, J. S. Edgar, G. D. Jeffries, R. M. Lorenz, J. P. Shelby and D. T. Chiu, *Anal. Chem.*, 2005, 77, 1539–1544.

30 D. Irimia, R. G. Tompkins and M. Toner, *Anal. Chem.*, 2004, **76**, 6137–6143.

31 S. H. Kim, T. Yamamoto, D. Fourmy and T. Fujii, *Small*, 2011, 7, 3239–3247.

32 S. H. Kim, X. He, S. Kaneda, J. Kawada, D. Fourmy, H. Noji and T. Fujii, *Lab Chip*, 2014, **14**, 730–736.

33 W. C. Lee, S. Rigante, A. P. Pisano and F. A. Kuypers, *Lab Chip*, 2010, **10**, 2952–2958.

34 K. Eyer, P. Kuhn, C. Hanke and P. S. Dittrich, *Lab Chip*, 2012, **12**, 765–772.

35 K. Eyer, S. Stratz, P. Kuhn, S. K. Kuster and P. S. Dittrich, *Anal. Chem.*, 2013, **85**, 3280–3287.

36 I. K. Dimov, R. Lu, E. P. Lee, J. Seita, D. Sahoo, S. M. Park, I. L. Weissman and L. P. Lee, *Nat. Commun.*, 2014, **5**, 3451.

37 A. K. White, M. VanInsberghe, O. I. Petriv, M. Hamidi, D. Sikorski, M. A. Marra, J. Piret, S. Aparicio and C. L. Hansen, *Proc. Natl. Acad. Sci. U. S. A.*, 2011, **108**, 13999–14004.

38 D. R. Albrecht, G. H. Underhill, T. B. Wassermann, R. L. Sah and S. N. Bhatia, *Nat. Methods*, 2006, **3**, 369–375.

39 Y. Chen, T. H. Wu, Y. C. Kung, M. A. Teitell and P. Y. Chiou, *Analyst*, 2013, **138**, 7308–7315.

40 S. H. Kim, M. Antfolk, M. Kobayashi, S. Kaneda, T. Laurell and T. Fujii, *Lab Chip*, 2015, **15**, 4356–4363.